

---

# AUTO-ENCODING GOODNESS OF FIT

Aaron Palmer<sup>1</sup>, Zhiyi Chi<sup>2</sup>, Derek Aguiar<sup>1</sup>, Jinbo Bi<sup>1</sup>

<sup>1</sup>Department of Computer Science and Engineering, University of Connecticut

<sup>2</sup>Department of Statistics, University of Connecticut

{aaron.palmer, zhiyi.chi, derek.aguiar, jinbo.bi}@uconn.edu

## ABSTRACT

For generative autoencoders to learn a meaningful latent representation for data generation, a careful balance must be achieved between reconstruction error and how close the distribution in the latent space is to the prior. However, this balance is challenging to achieve due to a lack of criteria that work both at the mini-batch (local) and aggregated posterior (global) level. Goodness of fit (GoF) hypothesis tests provide a measure of statistical indistinguishability between the latent distribution and a target *distribution class*. In this work, we develop the Goodness of Fit Autoencoder (GoFAE), which incorporates hypothesis tests at two levels. At the mini-batch level, it uses GoF test statistics as regularization objectives. At a more global level, it selects a regularization coefficient based on higher criticism, i.e., a test on the uniformity of the local GoF p-values. We justify the use of GoF tests by providing a relaxed  $L_2$ -Wasserstein bound on the distance between the latent distribution and target prior. We propose to use GoF tests and prove that optimization based on these tests can be done with stochastic gradient (SGD) descent on a compact Riemannian manifold. Empirically, we show that our higher criticism parameter selection procedure balances reconstruction and generation using mutual information and uniformity of p-values respectively. Finally, we show that GoFAE achieves comparable FID scores and mean squared errors with competing deep generative models while retaining statistical indistinguishability from Gaussian in the latent space based on a variety of hypothesis tests.

## 1 INTRODUCTION

Training generative autoencoders (GAEs) to generate quality samples requires balancing low reconstruction error with a regularization loss that encourages the latent representation to be meaningful for data generation (Hinton & Salakhutdinov, 2006; Ruthotto & Haber, 2021). Variational autoencoders (VAEs) achieve this balance by maximizing a lower bound on the data log-likelihood, which consists of a reconstruction term and a Kullback-Leibler (KL) divergence term between the posterior and prior distributions (Kingma & Welling, 2013; Rezende et al., 2014). The development of new GAE *meta-priors* (Bengio et al., 2013) generalizes assumptions about the data distribution in the latent space and have enabled the learning of representations that are hierarchically organized (Sønderby et al., 2016; Vahdat & Kautz, 2020), semi-supervised (Kingma et al., 2014), clustered (Makhzani et al., 2015; Lechat et al., 2021), or disentangled (Kumar et al., 2018; Horan et al., 2021). Meta-priors are typically enforced with an additive term in the GAE loss function that minimizes a statistical distance, e.g., KL divergence, between the posterior and a specific prior (Tschannen et al., 2018).

Another important class of statistical distances used in GAE meta-priors are based on optimal transport (OT) and Wasserstein distance, including the Wasserstein (WAE) (Tolstikhin et al., 2017), Sinkhorn (Patrini et al., 2018) and sliced-Wasserstein autoencoders (SWAE) (Kolouri et al., 2018). Importantly, OT-based GAEs encourage the *aggregated* posterior density to match an assumed prior distribution (compared to, e.g., VAEs that typically minimize the per-sample discrepancy) and have been shown to avoid the disadvantages of VAEs and adversarial methods (Tolstikhin et al., 2017). However, in all cases, a balance between reconstruction and generation is required (Alemi et al., 2018) to prevent decoupling between the posterior and the prior (Hoffman & Johnson, 2016) or vanishing KL between the two (Bowman et al., 2016). Regardless of the selected meta-prior, it is difficult to decide when the posterior is *close enough* to the prior due to: (a) the absence of tight constraints on

the statistical distances; (b) their distributions across mini-batches; and (c) the difference in scale between reconstruction and regularization objectives. If the posterior deviates from the prior, GAEs may generate samples of poor quality or with incorrect proportions (Rubenstein et al., 2018).

In contrast to statistical distances, goodness-of-fit (GoF) tests are statistical hypothesis tests that measure the indistinguishability between the posterior and a prior *distribution class* (Stephens, 2017), typically the class of Gaussians. While both parametric (Ridgeway & Mozer, 2018; Palmer et al., 2018) and nonparametric (Ding et al., 2019) hypothesis tests have been used in GAEs, prior work exhibits both theoretical and practical issues. In GAEs, GoF test statistics are optimized *locally* in mini-batches and no mechanism exists to determine if the *aggregated* posterior is indistinguishable from the prior. If GoF test p-values are small (i.e., mini-batches are distinguishable from the prior), then sampling quality is poor; conversely, an abundance of large GoF p-values may result in poor reconstruction as the posterior matches too closely to the prior at the mini-batch level (Lucas et al., 2019). Careful selection of regularization coefficients is required to ensure that the statistical distance is *close enough* but *not too close* to balance reconstruction and generation. Further, test statistic optimization in GAEs suffers from identifiability issues, unbounded domains, and gradient singularities and there exists no principled algorithm to optimize GoF using SGD.

**Our Contributions:** We develop and justify a framework for parametric test statistic optimization, resulting in a novel GAE that optimizes GoF tests for normality, and an algorithm for regularization coefficient selection based on p-value higher criticism (Donoho et al., 2004). Note that the GoF tests are not only for Gaussians with nonsingular covariance matrices, but *all* Gaussians, so they can handle situations where the data distribution is concentrated on or closely around a manifold with dimension smaller than the ambient space. The framework uses Gaussian priors as it is a standard option [(Doersch, 2016; Bousquet et al., 2017; Kingma et al., 2019)], and also because normality tests are much better understood than GoF tests for other distributions, with many more tests and more accurate calculation of p-values available. The framework can be modified to use other priors in a straightforward way provided that the same level of understanding can be gained on GoF tests for those priors as for normality tests. All proofs are deferred to the appendix. Specifically, our contributions are summarized as follows.

- We propose a framework (Sec. 2) for bounding the statistical distance between the posterior and the prior in GAEs, which forms the theoretical foundation for a deterministic GAE - Goodness of Fit Autoencoder (GoFAE), that directly optimizes GoF hypothesis test statistics.
- We examine four GoF tests of normality based on correlation and empirical distribution functions (Sec. 3). Each GoF test focuses on a different aspect of Gaussianity, e.g., moments or quantiles.
- A model selection method using higher criticism of p-values is proposed (Sec. 3), which enables global normality testing of the aggregated posterior and is test-based instead of performance-based. This method helps determine the range of the regularization coefficient that well balances reconstruction and generation using uniformity of p-values respectively (Fig. 2b).
- We show that gradient based optimization of test statistics for normality can be complicated by identifiability issues, unbounded domains, and gradient singularities; we propose a SGD that optimizes over a Riemannian manifold (Stiefel manifold in our case) that effectively solves our GAE formulation with convergence analysis (Sec. 4).
- We show that GoFAE achieves comparable FID scores and mean squared error on three datasets while retaining statistical indistinguishability from Gaussian in the latent space (Sec. 5).

## 2 A GENERATIVE AUTO-ENCODER FRAMEWORK

Let  $(\mathcal{X}, \mathbb{P}_X)$  and  $(\mathcal{Z}, \mathbb{P}_Z)$  be two probability spaces. In our setup,  $\mathbb{P}_X$  is the true, but unknown, data distribution while  $\mathbb{P}_Z$  is a pre-specified, or prior distribution on the latent space  $\mathcal{Z}$ .<sup>1</sup> An implicit generative model aims to find a possibly stochastic mapping  $G : \mathcal{Z} \rightarrow \mathcal{X}$ , known as the decoder, such that the distribution of  $G(Z)$ , i.e.,  $\mathbb{P}_{G(Z)}$  matches  $\mathbb{P}_X$ , where  $Z \sim \mathbb{P}_Z$ . One approach is based on optimal transport (OT) (Villani, 2008). Recall that if  $\mu$  and  $\nu$  are two distributions on a space  $\mathcal{E}$  and  $c(u, v)$  is a cost function on  $\mathcal{E}$ , then the OT cost to transfer  $\mu$  to  $\nu$  is  $\mathcal{T}_c(\mu, \nu) = \inf_{\pi \in \Pi(\mu, \nu)} \mathbb{E}_{(U, V) \sim \pi} [c(U, V)]$ , where  $\Pi(\mu, \nu)$  is the set of all joint probability distributions with marginals  $\mu$  and  $\nu$ . If  $\mathcal{E}$  is endowed with a metric  $d$  and  $c(u, v) = d(u, v)^p$  with  $p > 0$ , then  $d_{W_p}(\mu, \nu) = \mathcal{T}_c(\mu, \nu)^{1/p}$  is known as the  $L_p$ -Wasserstein distance. In principle, the decoder  $G$  can

<sup>1</sup>This should be distinguished from the priors in Bayesian statistics.

be learned by solving  $\min_G \mathcal{T}_c(\mathbb{P}_X, \mathbb{P}_{G(Z)})$ . Unfortunately, the minimization is intractable. Instead, the idea of the autoencoder approach is to find a possibly stochastic mapping  $F : \mathcal{X} \rightarrow \mathcal{Z}$ , known as the encoder, such that the distribution of  $Y = F(X)$ , i.e.,  $\mathbb{P}_Y$  matches the prior  $\mathbb{P}_Z$ . This idea combined with the generative modeling leads to GAEs, which learn the encoder and decoder by solving the following optimization problem

$$\min_{F, G} [\mathbb{E}_{X \sim \mathbb{P}_X, Y = F(X)} c(X, G(Y)) + \lambda D(\mathbb{P}_Y, \mathbb{P}_Z)], \quad (1)$$

where  $\lambda > 0$  is a regularization coefficient and  $D$  is a penalty on statistical discrepancy. In the GAE framework,  $Y = F(X)$  is the latent variable or code with  $\mathbb{P}_Y$  referred to as the aggregated posterior,  $G(Y) = G(F(X))$  the reconstruction of  $X$ , and  $G(Z)$  the generated data. When  $\mathcal{X}$  and  $\mathcal{Z}$  are Euclidean spaces, a common choice for  $c$  is the squared Euclidean distance, leading to the  $L_2$ -Wasserstein distance  $d_{W_2}$  and the following bounds.

**Proposition 1.** *If  $\mathcal{X}$  and  $\mathcal{Z}$  are Euclidean spaces and the decoder  $G$  is differentiable, then (a)  $d_{W_2}(\mathbb{P}_{G(Y)}, \mathbb{P}_{G(Z)}) \leq \|\nabla G\|_\infty d_{W_2}(\mathbb{P}_Y, \mathbb{P}_Z)$ , (b)  $d_{W_2}(\mathbb{P}_X, \mathbb{P}_{G(Z)}) \leq [\mathbb{E}\|X - G(Y)\|^2]^{1/2} + \|\nabla G\|_\infty d_{W_2}(\mathbb{P}_Y, \mathbb{P}_Z)$ .*

Combined with the triangle inequality for  $d_{W_2}$ , (a) and (b) imply that when the reconstruction error  $[\mathbb{E}\|X - G(Y)\|^2]^{1/2}$  is small, proximity between the latent distribution  $\mathbb{P}_Y$  and the prior  $\mathbb{P}_Z$  is sufficient to ensure proximity of the generated data distribution  $\mathbb{P}_{G(Z)}$  and the data distribution  $\mathbb{P}_X$ . Both (a) and (b) are similar to (Patrini et al., 2018), though here a less tight bound – the square-error – is used in (b) as it is an easier objective to optimize. In practice the encoder and decoder are networks trained using mini-batches of data. Henceforth, we denote them by  $F_\theta$  and  $G_\phi$  respectively, with  $\theta$  and  $\phi$  being the parameters of the corresponding networks. Given a mini-batch of size  $m$ ,  $\{X_i\}_{i=1}^m$ , the  $L_2$ -Wasserstein distance between the empirical distribution of  $\{Y_i = F_\theta(X_i)\}_{i=1}^m$  and  $\mathbb{P}_Z$  is a natural approximation of  $d_{W_2}(\mathbb{P}_Y, \mathbb{P}_Z)$  because it is a consistent estimator of the latter as  $m \rightarrow \infty$ , although in general is biased (Xu et al., 2020).

**Proposition 2.** *Let  $\hat{\mathbb{P}}_{X,m}$  be the empirical distribution of samples  $\{X_i\}_{i=1}^m$ , and  $\hat{\mathbb{P}}_{Y,m}$  be the empirical distribution of  $\{Y_i = F_\theta(X_i)\}_{i=1}^m$ . Assume that  $F_\theta(X)$  is differentiable with respect to  $X$  with bounded gradients  $\nabla F_\theta(X)$ . Then, (a)  $d_{W_2}(\hat{\mathbb{P}}_{Y,m}, \mathbb{P}_Y) \leq \|\nabla F_\theta\|_\infty d_{W_2}(\hat{\mathbb{P}}_{X,m}, \mathbb{P}_X)$ , (b)  $d_{W_2}(\mathbb{P}_Y, \mathbb{P}_Z) \leq d_{W_2}(\hat{\mathbb{P}}_{Y,m}, \mathbb{P}_Z) + \|\nabla F_\theta\|_\infty d_{W_2}(\hat{\mathbb{P}}_{X,m}, \mathbb{P}_X)$ .*

For reasonably large  $m$ ,  $d_{W_2}(\hat{\mathbb{P}}_{X,m}, \mathbb{P}_X)$  is small, so from (b), the proximity of the latent distribution and the prior is mainly controlled by the proximity between the empirical distribution  $\hat{\mathbb{P}}_{Y,m}$  and  $\mathbb{P}_Z$ . Together with Proposition 1, this shows that in order to achieve close proximity between  $\mathbb{P}_{G(Z)}$  and  $\mathbb{P}_X$ , we need to have a strong control on the proximity between  $\hat{\mathbb{P}}_{Y,m}$  and  $\mathbb{P}_Z$  in addition to a good reconstruction. To this end, we propose to use hypothesis tests (HTs) associated with the Wasserstein distance. Note that HTs associated with other statistical distances can also be used in conjunction. Many standard statistical distances are not metric. We will consider several well-known tests, including the Shapiro-Wilk (SW) test (Shapiro & Wilk, 1965). While the SW aims to control the Wasserstein distance, the other tests aim to control statistical distances dominated by the Wasserstein distance. Although at the *population* level, the Wasserstein distance provides stronger separation between different distributions, at the *sample* level, noisy data can exhibit various properties that some tests are sensitive to while others are not. Therefore, it is useful to exploit different tests.

### 3 THE NEED FOR A HIGHER CRITICISM: FROM LOCAL TO GLOBAL TESTING

GoF tests assess whether a sample of data,  $\{Y_i\}_{i=1}^m$ , is drawn from a distribution class  $\mathcal{G}$ . The most general opposing hypotheses are  $\mathcal{H}_0 : \mathbb{P}_Y \in \mathcal{G}$  vs  $\mathcal{H}_1 : \mathbb{P}_Y \notin \mathcal{G}$ . A test is specified by a test statistic  $T$  and a significance level  $\alpha \in (0, 1)$ . The observed value of the statistic is  $T(\{Y_i\}_{i=1}^m)$  and its (lower tail) p-value is  $P(T \leq T(\{Y_i\}_{i=1}^m) | \mathcal{H}_0)$ .  $\mathcal{H}_0$  is rejected in favor of  $\mathcal{H}_1$  at level  $\alpha$  if the p-value is less than  $\alpha$ , or equivalently, if  $T(\{Y_i\}_{i=1}^m) \leq T_\alpha$ , where  $T_\alpha$  is the  $\alpha$ -th quantile of  $T$  under  $\mathcal{H}_0$ . The probability integral transform (PIT) states that if  $T$  has a continuous distribution under  $\mathcal{H}_0$ , the p-values are uniformly distributed on  $(0, 1)$  (Murdoch et al., 2008). Multivariate normality (MVN) has received the most attention in the study on multivariate GoF tests. A random variable  $Y \in \mathbb{R}^d$  has a normal distribution if and only if for every  $\mathbf{u} \in \mathcal{S}$ ,  $Y^T \mathbf{u}$ , the projection of  $Y$  on  $\mathbf{u}$ , follows a UVN distribution (Rao et al., 1973), where  $\mathcal{S} = \{\mathbf{u} \in \mathbb{R}^d \mid \|\mathbf{u}\| = 1\}$  is the unit sphere in  $\mathbb{R}^d$ .

Furthermore, if  $Y$  has a non-normal distribution, the set of  $\mathbf{u} \in \mathcal{S}$  with  $Y^T \mathbf{u}$  being normal has Lebesgue measure 0 (Shao & Zhou, 2010). Thus to test on MVN, one way is to apply GoF tests on univariate normality (UVN) to a set of (random) projections of  $Y$  and then make a decision based on the resulting collection of test statistics. Many univariate tests exist (Looney, 1995; Mecklin & Mundfrom, 2005), each focusing on different distributional characteristics. Recently, GoF tests based on reproducing kernel Hilbert space theory have been developed (Liu et al., 2016; Chwialkowski et al., 2016). In this work, we only use traditional GoF tests. We next briefly describe correlation based (CB) tests because they are directly related to the Wasserstein distance. For other test types, see appendix §B. In essence, CB tests on UVN (Dufour et al., 1998) are based on assessment of the correlation between empirical and UVN quantiles. Two common CB tests are Shapiro-Wilk (SW) and Shapiro-Francia (SF) (Shapiro & Francia, 1972). Their test statistics will be denoted by  $T_{SW}$  and  $T_{SF}$  respectively. Both are closely related to  $d_{W_2}$ . For example, for  $m \gg 1$ ,  $T_{SW}$  is a strictly decreasing function of  $d_{W_2}(\mathbb{P}_{Y,m}, \mathcal{N}(0, 1))$  (del Barrio et al., 1999), i.e., large  $T_{SW}$  values correspond to small  $d_{W_2}$ , justifying the rule that  $T_{SW} > T_\alpha$  in order *not* to reject  $\mathcal{H}_0$ .

**The Benefits of GoF Testing in Autoencoders.** GoF tests on MVN inspect if  $\mathbb{P}_Y$  is equal to some  $\mathbb{P}_Z \in \mathcal{G}$ , where  $\mathcal{G}$  is the class of all Gaussians, i.e., MVN distributions. The primary justification for preferring  $\mathbb{P}_Z$  as a Gaussian to the more commonly specified isotropic Gaussian (Makhzani et al., 2015; Kingma & Welling, 2013; Higgins et al., 2017; Dai & Wipf, 2019) is that its covariance  $\Sigma$  is allowed to implicitly adapt during training. For example,  $\Sigma$  can be of full rank, allowing for correlations between the latent variables, or singular (i.e., a degenerate MVN, Fig. S1). The ability to adapt to degenerate MVN is of particular benefit. If  $F_\theta$  is dif-

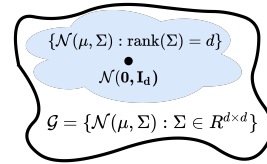


Figure 1: Illustration of distribution family  $\mathcal{G}$ .

ferentiable and the dimension of the latent space is greater than the intrinsic dimension of the data distribution, then the latent variable  $Y = F_\theta(X)$  only takes values in a manifold whose dimension is less than that of the latent space (Rubenstein et al., 2018). If  $\mathbb{P}_Z$  is only allowed to be an isotropic Gaussian, or more generally, a Gaussian with a covariance matrix of full rank, the regularizer in Eq. 1 will promote  $F_\theta$  that can fill the latent space with  $F_\theta(X)$ , leading to poor sample quality and wrong proportions of generated images (Rubenstein et al., 2018). Since GoF tests use the class  $\mathcal{G}$  of all Gaussians, they may help avoid such a situation. Note that this precludes the use of whitening, i.e. the transformation  $\Sigma^{-1/2}[\mathbf{X} - \mathbb{E}(\mathbf{X})]$  to get to  $\mathcal{N}(\mathbf{0}, \mathbf{I})$  as the covariance matrix  $\Sigma$  may be singular. In other words, whitening confines available Gaussians to a subset much smaller than  $\mathcal{G}$ ; see the cartoon Fig.( 1). Notably, a similar benefit was exemplified in the 2-Stage VAE, where decoupling manifold learning from learning the probability measure stabilized FID scores and sharpened generated samples when the intrinsic dimension is less than the dimension of the latent space (Dai & Wipf, 2019).

There are several additional benefits of GoF testing. First, it allows higher criticism (HC) to be used, a topic to be covered shortly. As mentioned in the introduction, GoF tests act at the local level (mini-batch), while HC applies to the aggregated level (training set). Second, many GoF tests produce closed-form test statistics, and thus do not require tuning and provide easily understood output. Lastly, testing for MVN via projections is unaffected by rank deficiency. This is *not* the case with the majority of multivariate GoF tests, e.g., the Henze-Zirkler test (Henze & Zirkler, 1990). In fact, any affine invariant test statistic for MVN must be a function of Mahalanobis distance, consequently requiring non-singularity (Henze, 2002).

### 3.1 A LOCAL PERSPECTIVE: GOODNESS OF FIT FOR NORMALITY

In light of Section 2, the aim is to ensure the proximity of the data distribution  $\mathbb{P}_X$  and the distribution  $\mathbb{P}_{G(Z)}$  by finding  $F_\theta, G_\phi$  such that the reconstruction error is small and the distribution  $\mathbb{P}_Y$  of the latent variable  $Y = F_\theta(X)$  matches the prior  $\mathbb{P}_Z$ . If the prior is taken to be in  $\mathcal{G}$ , then given a reconstruction loss function  $d$ , we can formulate the problem as  $\min_{\theta, \phi} \mathbb{E}[d(X, G_\phi(Y))]$  s.t.  $Y = F_\theta(X)$  is Gaussian. To enforce the constraint in the minimization, a HT can be conducted to decide whether or not to reject the null  $\mathcal{H}_0 : \mathbb{P}_{F_\theta(X)} \in \mathcal{G}$ . Without loss of generality, suppose that we use a test statistic  $T$  such that  $\mathcal{H}_0$  is rejected when  $T$  is *small*. It is natural to include the rejection criterion as a constraint to the optimization problem  $\min_{\theta, \phi} \mathbb{E}[d(X, G_\phi(Y))]$ , s.t.  $\mathbb{E}[T(F_\theta(X))] > T_\alpha$ . Rewriting with regularization coefficient  $\lambda$  leads to the Lagrangian  $\min_{\theta, \phi} \mathbb{E}[d(X, G_\phi(Y))] + \lambda(T_\alpha - \mathbb{E}[T(F_\theta(X))])$ . Since  $\lambda \geq 0$ , the final objective can be simplified to  $\min_{\theta, \phi} \mathbb{E}[d(X, G_\phi(Y)) - \lambda T(F_\theta(X))]$ .

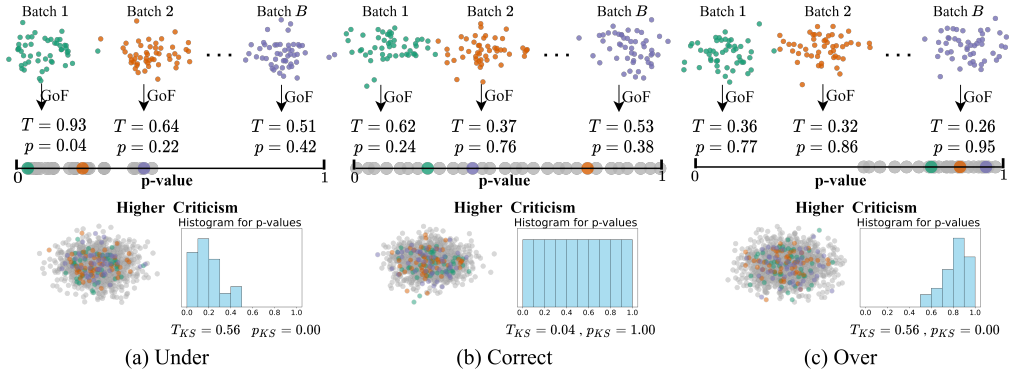


Figure 2: Demonstration of model selection. When the regularization coefficient  $\lambda$  is too small (a) or too big (c), GAE is under (or over) regulated, resulting in large values of higher criticism (shown here an example of Kolmogorov–Smirnov (KS) test  $T_{KS}$  of the uniformity of GoF test p-values over all mini-batches. (b) shows the case when an appropriate  $\lambda$  is chosen with a small  $T_{KS}$  value.

When the network is trained using a *single* mini-batch of size  $m$ , making  $Y$  *less* statistically distinguishable from  $\mathcal{G}$  amounts to increasing  $\mathbb{E}[T(\{F_\theta(X_i)\}_{i=1}^m)]$ , where  $X_i$  are i.i.d.  $\sim \mathbb{P}_X$ . However, if the training results in none of the mini-batches yielding small  $T$  values to reject  $\mathcal{H}_0$  at a given  $\alpha$  level, it also indicates a mismatch between the latent and prior distributions. This type of mismatch cannot be detected at the mini-batch level; a more global view is detailed in the next section.

### 3.2 A GLOBAL PERSPECTIVE: GOODNESS OF FIT FOR UNIFORMITY - HIGHER CRITICISM

Neural networks are powerful universal function approximators (Hornik et al., 1989; Cybenko, 1989). With sufficient capacity it may be possible to train  $F_\theta$  to *overfit*, that is, to produce *too* many mini-batches with large p-values. Under  $\mathcal{H}_0$ , the PIT posits p-value uniformity. Therefore, it is expected that after observing many mini-batches, approximately a fraction  $\alpha$  of them will have p-values that are less than  $\alpha$ . This idea of a more encompassing test is known as Tukey’s higher criticism (HC) (Donoho et al., 2004). While *each* mini-batch GoF test is concerned with optimizing for indistinguishability from the prior distribution class  $\mathcal{G}$ , the HC test is concerned with testing whether the *collection* of p-values is uniformly distributed on  $(0, 1)$ , which may be accomplished through the Kolmogorov–Smirnov uniformity test. See Algorithm 1 for a pseudo-code and Fig. 2 for an illustration of the HC process. HC and GoF form a symbiotic relationship; HC cannot exist by itself, and GoF by itself may over or under fit, producing p-values in incorrect proportions.

#### Algorithm 1 Evaluating Higher Criticism

---

**Require:** Trained encoder  $F_\theta$ ,  $\{\mathbf{x}_i\}_{i=1}^N$ ,  
GoF test  $T$

- 1: **for**  $i = 1 : \lfloor N/m \rfloor$  **do**
- 2:     Randomly sample mini-batch  $\mathbf{X}$  of size  $m$
- 3:      $\mathbf{Y} = G_\theta(\mathbf{X})$
- 4:     **if** projection required **then**
- 5:          $T^* = T(\mathbf{Y}\mathbf{u})$ , where  $\mathbf{u} \in \mathcal{S}$
- 6:     **else**
- 7:          $T^* = T(\mathbf{Y})$
- 8:     Calculate p-value of  $T^*$  and store it
- 9: Use KS to evaluate uniformity of p-value set

---

## 4 RIEMANNIAN SGD FOR OPTIMIZING A GOODNESS OF FIT AUTOENCODER

A GoF test statistic  $T$  is not merely an evaluation mechanism. Its gradient will impact how the model learns what characteristics of a sample indicate strong deviation from normality, carrying over to what the aggregated posterior  $\mathbb{P}_Y$  becomes. The following desiderata may help when selecting  $T$ . In the following, we denote a collection of sample observations by bold  $\mathbf{X}$ ,  $\mathbf{V}$ , and  $\mathbf{Y}$ .

- **HT-Trainable:**  $T(F_\theta(\mathbf{X}))$  is almost everywhere continuously differentiable in feasible region  $\Omega$ .
- **HT-Consistent:** There exists a  $\theta^*$  in  $\Omega$  such that  $F_{\theta^*}(\mathbf{X})$  becomes indistinguishable from the target distribution in the sense that  $\mathcal{H}_0$  cannot be rejected.

HT-Trainable is needed if gradient based methods are used to optimize the network parameters. Consider a common encoder architecture  $F_\theta$  that consists of multiple feature extraction layers (forming a mapping  $H_\Xi(\mathbf{X})$ ) followed by a fully connected layer with parameter  $\Theta$ . Thus,  $F_\theta(\mathbf{X}) =$

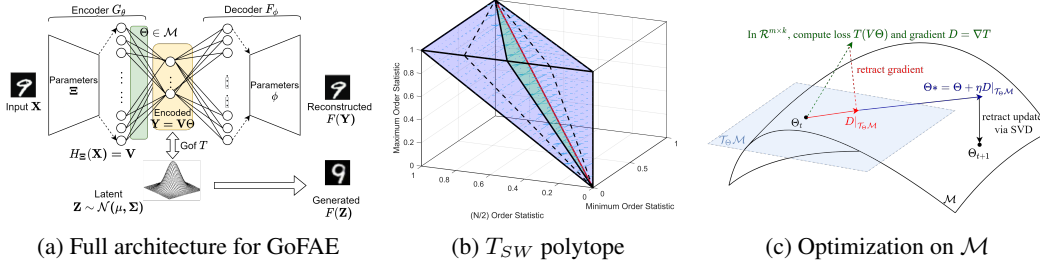


Figure 3: (a) GoFAE Architecture. (b) Example of singularity. Blue region is a polytope created as  $\mathcal{U} = \{\mathbf{x} = [x_1, x_2, x_3] \in \mathbb{R}^3 : 0 \leq x_1 \leq x_2 \leq x_3 \leq 1\}$ . For  $\forall \mathbf{x} \in \mathcal{U}$ , the coordinates of  $\mathbf{x}$  are also its order statistics, the min, median and max coordinates corresponds to the  $x, y$  and  $z$ -axis. The green simplex is where  $T_{SW}(\{x_1, x_2, x_3\}) = 1$ , and the region built with the dotted lines and the red line creates an acceptance region, outside of which is the rejection region. The light blue arrows are the derivatives at corresponding points and the red boundary line corresponds to the singularity where the gradient blows up. (c) Visualization for GoF optimization on a Stiefel manifold  $\mathcal{M}$ .

$H_\Xi(\mathbf{X})\Theta = \mathbf{V}\Theta = \mathbf{Y}$ , and  $\theta = \{\Xi, \Theta\}$ . The last layer is linear with no activation function as shown in Fig. 3a. With this design, normality can be optimized with respect to the last layer  $\Theta$  as discussed below. Given an HT-Consistent statistic  $T$ , it is natural to seek a solution,  $\theta^*$ .

**Theorem 3.** Suppose  $\mathbf{V} \in \mathbb{R}^{m \times k}$  is of full row rank. For  $\Theta \in \mathbb{R}^{k \times d}$ , define  $\mathbf{Y} = \mathbf{V}\Theta$ . Denote  $T_{SW} = T_{SW}(\mathbf{Y}\mathbf{u})$  where  $\mathbf{u} \in \mathbb{R}^d$  is a unit vector. Then,  $T_{SW}$  is differentiable with respect to  $\Theta$  almost everywhere, and  $\nabla_\Theta T_{SW} = \mathbf{0}$  if and only if  $T_{SW} = 1$ .

This theorem justifies the use of  $T_{SW}$  as an objective function according to HT-Conditions. The largest possible value of  $T_{SW}$  is 1, corresponding to an inability to detect deviation from normality no matter what level  $\alpha$  is specified. See the appendix for other HT choices.

**Identifiability, Singularities, and Stiefel Manifold.** If  $\mathbf{Y} = \mathbf{V}\Theta$  is Gaussian for some  $\Theta$ , then  $\mathbf{V}\Theta\mathbf{M}$  is also Gaussian for any nonsingular matrix  $\mathbf{M}$ . Thus, any matrix of the form  $\Theta\mathbf{M}$  is a solution. This leads to several problems when optimizing an objective function containing  $\Theta$  as a variable and the test statistic as part of the objective. First, there is an identifiability issue since, without any restrictions, the set of solutions is infinite. Here, all that matters is the direction of the projection, so restricting the space to the unit sphere is reasonable. Second, almost all GoF tests for normality in the current literature are affine invariant. However, the gradient and Hessian of the test statistics will not be bounded. Fig. 3b illustrates an example of such a singularity issue.

**Theorem 4.** Let  $T(\{\mathbf{y}_i\}_{i=1}^m)$ ,  $m \geq 3$  be any affine invariant test statistic that is non-constant and differentiable wherever  $\mathbf{y}_i$  are not all equal. Then, for any  $\mathbf{b}$ , as  $(\mathbf{y}_1, \dots, \mathbf{y}_m) \rightarrow (\mathbf{b}, \dots, \mathbf{b})$ ,  $\sup \|\nabla T(\{\mathbf{y}_i\}_{i=1}^m)\| \rightarrow \infty$ , where  $\|\cdot\|$  is the Frobenius norm.

If  $\Theta$  is searched without being kept away from zero or the diagonal line, traditional SGD results will not be applicable to yield convergence of  $\Theta$ . A common strategy might be to lower bound the smallest singular value of  $\Theta^T \Theta$ . However, it does not solve the issue that any re-scaling of  $\Theta$  leads to another solution, so  $\Theta$  must be also upper bounded. It is thus desirable to restrict  $\Theta$  in such a way that avoids getting close to singular by both upper and lower bounding it in terms of its singular values. We propose to restrict  $\Theta$  to the compact Riemannian manifold of orthonormal matrices, i.e.  $\Theta \in \mathcal{M} = \{\Theta \in \mathbb{R}^{k \times d} : \Theta^T \Theta = \mathbf{I}_d\}$  which is also known as the Stiefel manifold. This imposes a feasible region for  $\theta \in \Omega = \{\{\Xi, \Theta\} : \Theta^T \Theta = \mathbf{I}_d\}$ . Optimization over a Stiefel manifold has been studied previously (Nishimori & Akaho, 2005; Absil et al., 2009; Cho & Lee, 2017; Bécigneul & Ganea, 2018; Huang et al., 2018; 2020; Li et al., 2020).

#### 4.1 OPTIMIZING GOODNESS OF FIT TEST STATISTICS

A Riemannian metric provides a way to measure lengths and angles of tangent vectors of a smooth manifold. For the Stiefel manifold  $\mathcal{M}$ , in the Euclidean metric, we have  $\langle \Gamma_1, \Gamma_2 \rangle = \text{trace}(\Gamma_1^T \Gamma_2)$  for any  $\Gamma_1, \Gamma_2$  in the tangent space of  $\mathcal{M}$  at  $\Theta$ ,  $\mathcal{T}_\Theta \mathcal{M} = \{\Gamma : \Gamma^T \Theta + \Theta^T \Gamma = \mathbf{0}, \Theta \in \mathcal{M}\}$  (Li et al., 2020). For arbitrary matrix  $\Theta \in \mathbb{R}^{k \times d}$ , the retraction back to  $\mathcal{M}$ , denoted

$\Theta|_{\mathcal{M}}$ , can be performed via a singular value decomposition (SVD),  $\Theta|_{\mathcal{M}} = \mathbf{R}\mathbf{S}^T$ , where  $\Theta = \mathbf{R}\mathbf{A}\mathbf{S}^T$  and  $\mathbf{A}$  is the  $d \times d$  diagonal matrix of singular values,  $\mathbf{R} \in \mathbb{R}^{k \times d}$  has orthonormal columns, i.e.  $\mathbf{R} \in \mathcal{M}$ , and  $\mathbf{S} \in \mathbb{R}^{d \times d}$  is an orthogonal matrix. The retraction of the gradient  $\mathbf{D} = \nabla_{\Theta} T_*$  to  $\mathcal{T}_{\Theta}\mathcal{M}$ , denoted by  $\mathbf{D}|_{\mathcal{T}_{\Theta}\mathcal{M}}$ , can be accomplished by  $\mathbf{D}|_{\mathcal{T}_{\Theta}\mathcal{M}} = \mathbf{D} - \Theta(\Theta^T \mathbf{D} + \mathbf{D}^T \Theta)/2$  (Fig. 3c). The process of mapping Euclidean gradients to  $\mathcal{T}_{\Theta}\mathcal{M}$ , updating  $\Theta$ , and retracting back to  $\mathcal{M}$  is well known (Nishimori & Akaho, 2005). The next result states that the Riemannian gradient for  $T_{SW}$  has a finite second moment, which is needed for our convergence theorem in § 4.2.

**Theorem 5.** *Let  $T = T_{SW}$  be as in Theorem 3. Denote by  $\nabla_{\theta}$ ,  $\nabla_{\Theta}$ , the Riemannian gradient w.r.t.  $\theta$ ,  $\Theta$ , respectively, and  $\|\cdot\|$  the Frobenius norm. Let  $\mathbf{B} = (\mathbf{I} - \mathbf{J}/m)\mathbf{V}$ , i.e.,  $\mathbf{B}$  is obtained by subtracting from each row of  $\mathbf{V}$  the mean of the rows. Suppose (a)  $\sup_{\Xi}(\mathbb{E}[\|\mathbf{B}\|^4] + \mathbb{E}[\|\nabla_{\Xi}\mathbf{B}\|^4]) < \infty$ , and (b)  $\sup_{\|\mathbf{x}\|=1, \Xi} \mathbb{E}[\|\mathbf{B}\mathbf{x}\|^{-4}] < \infty$ . Then,  $\sup_{\theta} \mathbb{E}[\|\nabla_{\theta} T\|^2] < \infty$ .*

## 4.2 OPTIMIZING THE GOODNESS OF FIT AUTOENCODER

Given a mini-batch of size  $m$ ,  $\{\mathbf{x}_i\}_{i=1}^m$ , the GoFAE loss function is written as<sup>2</sup> :

$$\mathcal{L}(\theta, \phi; \{\mathbf{x}_i\}_{i=1}^m) = \frac{1}{m} \sum_{i=1}^m d(\mathbf{x}_i, G_{\phi}(F_{\theta}(\mathbf{x}_i))) \pm \lambda T(\{F_{\theta}(\mathbf{x}_i)\}_{i=1}^m), \quad (2)$$

where  $\theta = \{\Xi, \Theta\}$ . Since  $\Theta \in \mathcal{M}$ , model training requires Riemannian SGD. The proof of Bonnabel (2013) for the convergence of SGD on a Riemannian manifold, which extended from the Euclidean case (Bottou, 1998), requires conditions on step size, differentiability, and a uniform bound on the stochastic gradient. We show that this result holds under a much weaker condition, eliminating the need for a uniform bound. While we apply the resulting theorem to our specific problem with a Stiefel manifold, we emphasize that Theorem 6 is applicable to other suitable Riemannian manifolds.

**Theorem 6.** *Let  $\mathcal{M}$  be a connected Riemannian manifold with injectivity radius uniformly bounded from below by  $I > 0$ . Let  $C \in C^{(3)}(\mathcal{M})$  and  $R_w$  be a twice continuously differentiable retraction. Let  $z_0, z_1, \dots$  be i.i.d.  $\sim \zeta$  taking values in  $\mathcal{Z}$ . Let  $H : \mathcal{Z} \times \mathcal{M} \rightarrow \mathcal{TM}$  be a measurable function such that  $\mathbb{E}[H(\zeta, w)] = \nabla C(w)$  for all  $w \in \mathcal{M}$ , where  $\mathcal{TM}$  is the tangent bundle of  $\mathcal{M}$ . Consider the SGD update  $w_{t+1} = R_{w_t}(-\gamma_t H(z_t, w_t))$  with stepsize  $\gamma_t > 0$  satisfying  $\sum \gamma_t^2 < +\infty$  and  $\sum \gamma_t = +\infty$ . Suppose there exists a compact set  $K$  such that all  $w_t \in K$  and  $\sup_{w \in K} \mathbb{E}[\|H(\zeta, w)\|^2] \leq A^2$  for some  $A > 0$ . Then,  $C(w_t)$  converges almost surely and  $\nabla C(w_t) \rightarrow 0$  almost surely.*

In our context,  $C(\cdot)$  corresponds to Eq. (2). The parameters of GoFAE are  $\{\theta, \phi\} = \{\Xi, \Theta, \phi\}$  where  $\Xi, \phi$  are defined in Euclidean space, a Riemannian manifold endowed with the Euclidean metric, and  $\Theta$  on the Stiefel manifold. Therefore,  $\{\Xi, \Theta, \phi\}$  is a product manifold that is also Riemannian and  $\{\Xi, \Theta, \phi\}$  are updated simultaneously. Convergence of GoFAE holds from Proposition 5 and Theorem 6 provided that  $\Xi, \phi$  stay within a compact set. Algorithm 2 depicts the GoFAE pseudo-code.

## 5 EXPERIMENTS

We evaluate generation and reconstruction performance, normality, and informativeness of GoFAE using several GoF statistics on the MNIST (LeCun et al., 1998), CelebA (Liu et al., 2015) and CIFAR10 (Krizhevsky et al., 2009) datasets and compare to several other GAE models. We emphasize that our goal is not to merely to produce competitive evaluation metrics, but to provide a principled way to balance the reconstruction versus prior matching trade-off. For MNIST and CelebA the architectures are based on Tolstikhin et al. (2017), while CIFAR10 is from Lippe (2022). The aim is to keep the architecture consistent across models with the exception of method specific components. See the appendix for complete architectures (§C), training details (§D), and additional results (§E). The following results are from experiments on CelebA.

**Effect of  $\lambda$  and Mutual Information (MI).** We investigated the balance between generation and reconstruction in the GoFAE by considering mini-batch (local) GoF test p-value distributions, aggregated posterior (global) normality, and MI as a function of  $\lambda$  (Fig. 4). Global normality as assessed through the higher criticism (HC) principle for p-value uniformity denoted by  $KS_{unif}$  and computed using Algorithm 1. We trained GoFAE on CelebA using  $T_{SW}$  as the test statistic for  $\lambda = 10$  (Fig. 4a,

<sup>2</sup>The sign of  $\lambda$  is determined by the test statistic. Since  $T_{SW}$  is our exemplar it would be negative.

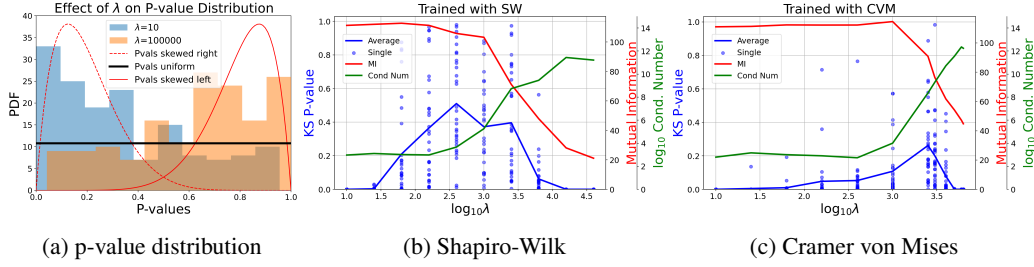


Figure 4: Effects of  $\lambda$  on p-value distribution and mutual information for GoFAE models.

blue) and  $\lambda = 100,000$  (Fig. 4a, yellow). For small  $\lambda$ , the model emphasizes reconstruction and the p-value distribution will be skewed right since the penalty for deviating from normality is small (Fig. 4a, red dashed line). As  $\lambda$  increases, more emphasis is placed on normality and, for some  $\lambda$ , p-values are expected to be uniformly distributed (Fig. 4a, black line). If  $\lambda$  is too large, the p-value distribution will be left-skewed (Fig. 4a, red solid line), which corresponds to overfitting the prior.

We assessed the normality of GoFAE mini-batch encodings, using 30 repetitions of Algorithm 1, for different  $\lambda$  and  $KS_{unif}$  (Figs. 4b-4c). The blue points and blue solid line represent the  $KS_{unif}$  test p-values and mean, respectively. HC rejects global normality ( $KS_{unif} < 0.05$ ) when the test statistic p-values are right-skewed (too many mini-batches deviate from normality) or left-skewed (mini-batches are *too* normal); this GoFAE property discourages the posterior from over-fitting the prior. The range of  $\lambda$  values for which the distribution of GoF test p-values is indistinguishable from uniform is where the mean  $KS_{unif} \geq 0.05$  (Figs. 4b-4c).

Finally, we used the estimated  $(\hat{\mu}, \hat{\Sigma})$  for each model to draw  $N = 10^4$  samples  $\{\mathbf{z}_i\}_{i=1}^N$  and generate images  $\{G_\phi(\mathbf{z}_i)\}_{i=1}^N$ . These images are then encoded, giving the set  $\{\tilde{\mathbf{z}}_i\}_{i=1}^N$  with  $\tilde{\mathbf{z}}_i = F_\theta(G_\phi(\mathbf{z}_i))$ , resulting in a Markov chain  $\{\mathbf{z}_i\}_{i=1}^N \rightarrow \{G_\phi(\mathbf{z}_i)\}_{i=1}^N \rightarrow \{\tilde{\mathbf{z}}_i\}_{i=1}^N$ . Assuming  $\tilde{\mathbf{z}}_i$  are also normal, the data processing inequality gives a lower bound on the MI (Figs. 4b-4c, red line). As  $\lambda$  increases the MI diminishes, suggesting the posterior overfits the prior as the encoding becomes independent of the data. The unimodality of the average  $KS_{unif}$  and monotonicity of MI suggests  $\lambda$  can be selected solely based on  $KS_{unif}$  without reference to a performance criterion.

**Gaussian Degeneracy.** Due to noise in the data, numerically the aggregate posterior can never be singular. Nevertheless, the experiments indicate that the GoF test can push the aggregated posterior to become “more and more singular” in the sense that the condition number of its covariance matrix,  $\kappa(\hat{\Sigma})$ , becomes increasingly large. As  $\lambda$  continues to increase,  $\kappa(\hat{\Sigma})$  also increases (Figs. 4b-4c, green line), implying a Gaussian increasingly concentrated around a lower-dimensional linear manifold. The same trend is shown in Fig.5, which depicts the spectrum of singular values (SV) of  $\hat{\Sigma}$  for each  $\lambda$  after training with  $T_{SW}$ . From the figure, it is seen that while the spectrum does not exhibit extremely large SVs, it has many small SVs. Notably in Figs. 4b-4c even when  $\lambda$  is not too large,  $\kappa(\hat{\Sigma})$  is relatively large, indicating a shift to lower-dimension. However, MI remains relatively large and the  $KS_{unif}$  test suggests the aggregated posterior is still indistinguishable from Gaussian. Together, these results are evidence that the GoFAE can adapt as needed to a reduced-dimension representation while maintaining the representation’s informativeness.

### Algorithm 2 GoFAE Optimization

**Require:** test  $T$ , learning rates:  $\eta_1, \eta_2$ , max iter.  $J$

- 1: **Initialize:**  $\Xi, \Theta, \phi$
- 2: **while**  $j < J$  **do**
- 3: Randomly sample mini-batch of size  $m$ ,  $\mathbf{X}$
- 4:  $\mathbf{V} = F_{\Xi_j}^{(1)}(\mathbf{X})$
- 5:  $\mathbf{Y} = F_{\Theta_j}^{(2)}(\mathbf{V}) = \mathbf{V}\Theta_j$
- 6: **if** test requires projection **then**
- 7:  $T^* = T(\mathbf{Y}\mathbf{u})$ , where  $\mathbf{u} \in \mathcal{S}$
- 8: **else**
- 9:  $T^* = T(\mathbf{Y})$
- 10:  $\mathcal{L} = d(\mathbf{X}, G_\phi(\mathbf{Y})) \pm \lambda T^*$
- 11:  $\Xi_{j+1} = \Xi_j - \eta_1 \nabla_{\Xi} \mathcal{L}$  or other optim
- 12:  $\phi_{j+1} = \phi_j - \eta_1 \nabla_{\phi} \mathcal{L}$  or other optim
- 13:  $\mathbf{D} = \nabla_{\Theta} T^*$
- 14:  $\Gamma = \mathbf{D}|_{\mathcal{T}_{\Theta, \mathcal{M}}} = \mathbf{D} - \Theta_j(\Theta_j^T \mathbf{D} + \mathbf{D}^T \Theta_j)/2$
- 15:  $\Theta'_{j+1} = \Theta_j + \eta_2 \Gamma$
- 16: Compute  $\mathbf{R}\mathbf{A}\mathbf{S}^T = \text{SVD}(\Theta'_{j+1})$
- 17:  $\Theta_{j+1} = \Theta'_{j+1}|_{\mathcal{M}} = \mathbf{R}\mathbf{S}^T$

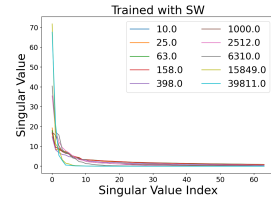


Figure 5: SV of  $\hat{\Sigma}$

Table 1: Evaluation of CelebA by MSE, FID scores, and samples with p-values from higher criticism.

Algorithm	MSE ↓	FID Score ↓		Kolmogorov-Smirnov Uniformity Test				
		Recon.	Gen.	SW	SF	CVM	KS	EP
AE-Baseline	69.32	40.28	126.43	0.0(0.0)	0.0(0.0)	0.0(0.0)	0.0(0.0)	0.0(0.0)
VAE (fixed $\gamma$ )	101.78	49.29	56.78	0.01(0.05)	0.0(0.01)	0.10(0.19)	0.30(0.30)	0.23(0.27)
VAE (learned $\gamma$ )	68.09	34.54	58.15	0.0(0.0)	0.0(0.0)	0.0(0.0)	0.0(0.0)	0.0(0.0)
2-Stage-VAE	68.09	34.54	49.55	0.51(0.26)	0.49(0.27)	0.49(0.29)	0.52(0.28)	0.49(0.32)
$\beta(10)$ -VAE	235.37	99.59	101.30	0.56(0.31)	0.46(0.35)	0.47(0.28)	0.38(0.25)	0.44(0.27)
$\beta(2)$ -VAE	129.72	60.72	65.65	0.19(0.21)	0.06(0.11)	0.42(0.29)	0.52(0.30)	0.44(0.27)
WAE-GAN	72.70	38.23	48.39	0.01(0.04)	0.0(0.0)	0.11(0.18)	0.14(0.19)	0.13(0.15)
GoFAE-SW(63)	<b>66.11</b>	34.69	43.76	0.14(0.23)	0.28(0.26)	0.01(0.03)	0.08(0.17)	0.08(0.17)
GoFAE-SF(25)	66.35	<b>33.89</b>	<b>43.3</b>	0.04(0.09)	0.12(0.20)	0.0(0.01)	0.02(0.04)	0.01(0.03)
GoFAE-CVM(398)	67.43	37.50	46.74	0.19(0.22)	0.34(0.29)	0.05(0.08)	0.16(0.27)	0.19(0.28)
GoFAE-KS(63)	66.62	35.14	43.93	0.0(0.00)	0.0(0.00)	0.0(0.00)	0.00(0.00)	0.00(0.00)
GoFAE-EP(10)	67.03	39.71	48.53	0.03(0.08)	0.06(0.10)	0.00(0.00)	0.00(0.00)	0.02(0.04)

**Reconstruction, Generation, and Normality.** We assessed the quality of the generated and test set reconstructed images using Fréchet Inception Distance (FID) (Heusel et al., 2017) and mean-square error (MSE) based on  $10^4$  samples (Table 1). We compared GoFAE with AE (Bengio et al., 2013), VAE (Kingma & Welling, 2013), VAE with learned  $\gamma$  (Dai & Wipf, 2019), 2-Stage VAE (Dai & Wipf, 2019),  $\beta$ -VAE (Higgins et al., 2017) and WAE-GAN (Tolstikhin et al., 2017); convergence was assessed by tracking the test set reconstruction error over training epochs (Tables S2–S8 and Fig. S9). Figs. 6a, 6b are for models presented in Table 1. We selected the smallest  $\lambda$  whose mean p-value of the HC uniformity test,  $KS_{unif}$ , was greater than 0.05 for GoFAE models. The CB GoF tests have the most competitive performance on FID and test set MSE. We assessed the normality of mini-batch encodings across each method using several GoF tests for normality combined with  $KS_{unif}$ . We ran 30 repetitions of Algorithm 1 for each method and reported the mean (std) of the  $KS_{unif}$  p-values in Table 1. In addition to superior MSE and FID scores, the GoFAE models obtained uniform p-values under varying GoF tests. Variability across GoF tests highlights the fact that different tests are sensitive to different distributional characteristics. Qualitative and quantitative assessments (§ E.3) and convergence plots (§ E.4) are given in the appendix for MNIST, CIFAR-10, and CelebA. Finally, an ablation study provided empirical justification for Riemannian SGD in the GoFAE (§ E.5).

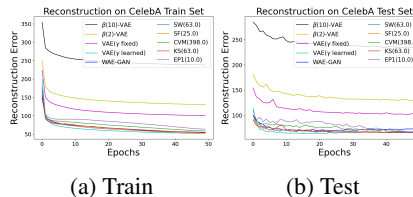


Figure 6: Convergence of reconstruction error on the CelebA training (a) and testing (b) sets.

## 6 SUMMARY AND CONCLUSION

We presented the GoFAE, a deterministic GAE based on optimal transport and Wasserstein distances that optimizes GoF hypothesis test statistics. We showed that gradient based optimization of GoFAE induces identifiability issues, unbounded domains, and gradient singularities, which we resolve using Riemannian SGD. By using GoF statistics to measure deviation from the prior *class* of Gaussians, our model is capable of implicitly adapting its covariance matrix during training from full-rank to singular, which we demonstrate empirically. We developed a performance agnostic model selection algorithm based on higher criticism of p-values for global normality testing of the aggregated posterior. Collectively, empirical results show that GoFAE achieves comparable reconstruction and generation performance while retaining statistical indistinguishability from Gaussian in the latent space.

Several limitations in our methods provide opportunities for future work. First, a most powerful GoF test for normality does not exist. Each test is sensitive to certain characteristics of the null distribution. In GAEs, the induced distribution is unknown; hence we can't know which test is best for the task. Solutions might include a weighted combination of tests or randomly selecting one for each iteration. Second, we solved difficulties in high-dimensional scaling of UVN GoF tests by projection, which can be slow for univariate tests because many samples from the unit sphere are required. Third, the increased interpretability of test statistic regularization comes with the danger of p-hacking by permuting the GoF test and regularization coefficient until significance is achieved (Head et al., 2015). This issue applies more broadly, can lead to biased and misleading findings, and possibly be used deceptively by wrongfully claiming statistical significance (Brodeur

---

et al., 2020); however, p-hacking can be detected with binomial tests (Gerber & Malhotra, 2008; Simmons et al., 2011), ameliorated by correcting for multiple comparisons (Streiner, 2015), or avoided with Bayesian posterior probabilities (Gelman & Loken, 2013). Lastly, the theoretical principles concerning overfitting while using a test statistic as a regularizer are not well understood and requires further investigation.

## REFERENCES

- P-A Absil, Robert Mahony, and Rodolphe Sepulchre. *Optimization algorithms on matrix manifolds*. Princeton University Press, 2009.
- Alexander Alemi, Ben Poole, Ian Fischer, Joshua Dillon, Rif A Saurous, and Kevin Murphy. Fixing a broken elbow. In *International Conference on Machine Learning*, pp. 159–168. PMLR, 2018.
- Gary Bécigneul and Octavian-Eugen Ganea. Riemannian adaptive optimization methods. *arXiv preprint arXiv:1810.00760*, 2018.
- Yoshua Bengio, Aaron Courville, and Pascal Vincent. Representation learning: A review and new perspectives. *IEEE transactions on pattern analysis and machine intelligence*, 35(8):1798–1828, 2013.
- Silvere Bonnabel. Stochastic gradient descent on riemannian manifolds. *IEEE Transactions on Automatic Control*, 58(9):2217–2229, 2013.
- Léon Bottou. Online learning and stochastic approximations. *On-line learning in neural networks*, 17(9):142, 1998.
- Olivier Bousquet, Sylvain Gelly, Ilya Tolstikhin, Carl-Johann Simon-Gabriel, and Bernhard Schölkopf. From optimal transport to generative modeling: the vegan cookbook. *arXiv preprint arXiv:1705.07642*, 2017.
- Samuel R. Bowman, Luke Vilnis, Oriol Vinyals, Andrew Dai, Rafal Jozefowicz, and Samy Bengio. Generating sentences from a continuous space. In *Proceedings of The 20th SIGNLL Conference on Computational Natural Language Learning*, pp. 10–21, Berlin, Germany, August 2016. Association for Computational Linguistics. doi: 10.18653/v1/K16-1002. URL <https://aclanthology.org/K16-1002>.
- Abel Brodeur, Nikolai Cook, and Anthony Heyes. Methods matter: P-hacking and publication bias in causal analysis in economics. *American Economic Review*, 110(11):3634–60, 2020.
- Minhyung Cho and Jaehyung Lee. Riemannian approach to batch normalization. In *Advances in Neural Information Processing Systems*, pp. 5225–5235, 2017.
- Kacper Chwialkowski, Heiko Strathmann, and Arthur Gretton. A kernel test of goodness of fit. In *International conference on machine learning*, pp. 2606–2615. PMLR, 2016.
- George Cybenko. Approximation by superpositions of a sigmoidal function. *Mathematics of control, signals and systems*, 2(4):303–314, 1989.
- Bin Dai and David Wipf. Diagnosing and enhancing vae models. *arXiv preprint arXiv:1903.05789*, 2019.
- Eustasio del Barrio, Juan A Cuesta-Albertos, Carlos Matrán, and Jesús M Rodríguez-Rodríguez. Tests of goodness of fit based on the l2-wasserstein distance. *Annals of Statistics*, pp. 1230–1239, 1999.
- Lizhong Ding, Mengyang Yu, Li Liu, Fan Zhu, Yong Liu, Yu Li, and Ling Shao. Two generator game: Learning to sample via linear goodness-of-fit test. In *Advances in Neural Information Processing Systems*, pp. 11260–11271, 2019.
- Carl Doersch. Tutorial on variational autoencoders. *arXiv preprint arXiv:1606.05908*, 2016.
- David Donoho, Jiashun Jin, et al. Higher criticism for detecting sparse heterogeneous mixtures. *The Annals of Statistics*, 32(3):962–994, 2004.

- 
- Jean-Marie Dufour, Abdeljelil Farhat, Lucien Gardiol, and Lynda Khalaf. Simulation-based finite sample normality tests in linear regressions. *The Econometrics Journal*, 1(1):154–173, 1998.
- Andrew Gelman and Eric Loken. The garden of forking paths: Why multiple comparisons can be a problem, even when there is no “fishing expedition” or “p-hacking” and the research hypothesis was posited ahead of time. *Department of Statistics, Columbia University*, 348, 2013.
- Alan S Gerber and Neil Malhotra. Publication bias in empirical sociological research: Do arbitrary significance levels distort published results? *Sociological Methods & Research*, 37(1):3–30, 2008.
- Megan L Head, Luke Holman, Rob Lanfear, Andrew T Kahn, and Michael D Jennions. The extent and consequences of p-hacking in science. *PLoS Biol*, 13(3):e1002106, 2015.
- N Henze and B Zirkler. A class of invariant consistent tests for multivariate normality. *Communications in Statistics-Theory and Methods*, 19(10):3595–3617, 1990.
- Norbert Henze. Invariant tests for multivariate normality: a critical review. *Statistical papers*, 43(4): 467–506, 2002.
- Martin Heusel, Hubert Ramsauer, Thomas Unterthiner, Bernhard Nessler, and Sepp Hochreiter. Gans trained by a two time-scale update rule converge to a local nash equilibrium. *arXiv preprint arXiv:1706.08500*, 2017.
- Irina Higgins, Loïc Matthey, Arka Pal, Christopher P. Burgess, Xavier Glorot, Matthew M. Botvinick, Shakir Mohamed, and Alexander Lerchner. beta-vae: Learning basic visual concepts with a constrained variational framework. In *ICLR*, 2017.
- Geoffrey E Hinton and Ruslan R Salakhutdinov. Reducing the dimensionality of data with neural networks. *science*, 313(5786):504–507, 2006.
- Matthew D Hoffman and Matthew J Johnson. Elbo surgery: yet another way to carve up the variational evidence lower bound. In *Workshop in Advances in Approximate Bayesian Inference, NIPS*, 2016.
- Daniella Horan, Eitan Richardson, and Yair Weiss. When is unsupervised disentanglement possible? *Advances in Neural Information Processing Systems*, 34, 2021.
- Kurt Hornik, Maxwell Stinchcombe, and Halbert White. Multilayer feedforward networks are universal approximators. *Neural networks*, 2(5):359–366, 1989.
- Lei Huang, Xianglong Liu, Bo Lang, Adams Yu, Yongliang Wang, and Bo Li. Orthogonal weight normalization: Solution to optimization over multiple dependent stiefel manifolds in deep neural networks. In *Proceedings of the AAAI Conference on Artificial Intelligence*, volume 32, 2018.
- Lei Huang, Xianglong Liu, Jie Qin, Fan Zhu, Li Liu, and Ling Shao. Projection based weight normalization: Efficient method for optimization on oblique manifold in dnns. *Pattern Recognition*, 105:107317, 2020.
- Diederik P Kingma and Max Welling. Auto-encoding variational bayes. *arXiv preprint arXiv:1312.6114*, 2013.
- Diederik P Kingma, Danilo J Rezende, Shakir Mohamed, and Max Welling. Semi-supervised learning with deep generative models. In *Proceedings of the 27th International Conference on Neural Information Processing Systems-Volume 2*, pp. 3581–3589, 2014.
- Diederik P Kingma, Max Welling, et al. An introduction to variational autoencoders. *Foundations and Trends® in Machine Learning*, 12(4):307–392, 2019.
- Soheil Kolouri, Phillip E Pope, Charles E Martin, and Gustavo K Rohde. Sliced-wasserstein autoencoder: An embarrassingly simple generative model. *arXiv preprint arXiv:1804.01947*, 2018.
- Alex Krizhevsky, Geoffrey Hinton, et al. Learning multiple layers of features from tiny images. 2009.
- Abhishek Kumar, Prasanna Sattigeri, and Avinash Balakrishnan. Variational inference of disentangled latent concepts from unlabeled observations. In *International Conference on Learning Representations*, 2018.

- 
- Alexis Lechat, Stéphane Herbin, and Frédéric Jurie. Semi-supervised class incremental learning. In *2020 25th International Conference on Pattern Recognition (ICPR)*, pp. 10383–10389. IEEE, 2021.
- Yann LeCun, Léon Bottou, Yoshua Bengio, and Patrick Haffner. Gradient-based learning applied to document recognition. *Proceedings of the IEEE*, 86(11):2278–2324, 1998.
- Jun Li, Li Fuxin, and Sinisa Todorovic. Efficient riemannian optimization on the stiefel manifold via the cayley transform. *arXiv preprint arXiv:2002.01113*, 2020.
- Phillip Lippe. UvA Deep Learning Tutorials. <https://uvadlc-notebooks.readthedocs.io/en/latest/>, 2022.
- Qiang Liu, Jason Lee, and Michael Jordan. A kernelized stein discrepancy for goodness-of-fit tests. In *International conference on machine learning*, pp. 276–284. PMLR, 2016.
- Ziwei Liu, Ping Luo, Xiaogang Wang, and Xiaoou Tang. Deep learning face attributes in the wild. In *Proceedings of the IEEE international conference on computer vision*, pp. 3730–3738, 2015.
- Stephen W Looney. How to use tests for univariate normality to assess multivariate normality. *The American Statistician*, 49(1):64–70, 1995.
- James Lucas, George Tucker, Roger B Grosse, and Mohammad Norouzi. Don’t blame the elbo! a linear vae perspective on posterior collapse. *Advances in Neural Information Processing Systems*, 32, 2019.
- Alireza Makhzani, Jonathon Shlens, Navdeep Jaitly, Ian Goodfellow, and Brendan Frey. Adversarial autoencoders. *arXiv preprint arXiv:1511.05644*, 2015.
- Christopher J Mecklin and Daniel J Mundfrom. A monte carlo comparison of the type i and type ii error rates of tests of multivariate normality. *Journal of Statistical Computation and Simulation*, 75(2):93–107, 2005.
- Duncan J Murdoch, Yu-Ling Tsai, and James Adcock. P-values are random variables. *The American Statistician*, 62(3):242–245, 2008.
- Yasunori Nishimori and Shotaro Akaho. Learning algorithms utilizing quasi-geodesic flows on the stiefel manifold. *Neurocomputing*, 67:106–135, 2005.
- Aaron Palmer, Dipak Dey, and Jinbo Bi. Reforming generative autoencoders via goodness-of-fit hypothesis testing. In *UAI*, pp. 1009–1019, 2018.
- Giorgio Patrini, Marcello Carioni, Patrick Forre, Samarth Bhargav, Max Welling, Rianne van den Berg, Tim Genewein, and Frank Nielsen. Sinkhorn autoencoders. *arXiv preprint arXiv:1810.01118*, 2018.
- Calyampudi Radhakrishna Rao, Calyampudi Radhakrishna Rao, Mathematischer Statistiker, Calyampudi Radhakrishna Rao, and Calyampudi Radhakrishna Rao. *Linear statistical inference and its applications*, volume 2. Wiley New York, 1973.
- Danilo Jimenez Rezende, Shakir Mohamed, and Daan Wierstra. Stochastic backpropagation and approximate inference in deep generative models. *arXiv preprint arXiv:1401.4082*, 2014.
- Karl Ridgeway and Michael C Mozer. Learning deep disentangled embeddings with the f-statistic loss. *Advances in Neural Information Processing Systems*, 31:185–194, 2018.
- Paul K Rubenstein, Bernhard Schoelkopf, and Ilya Tolstikhin. On the latent space of wasserstein auto-encoders. *arXiv preprint arXiv:1802.03761*, 2018.
- Lars Ruthotto and Eldad Haber. An introduction to deep generative modeling. *arXiv preprint arXiv:2103.05180*, 2021.
- Yongzhao Shao and Ming Zhou. A characterization of multivariate normality through univariate projections. *Journal of multivariate analysis*, 101(10):2637–2640, 2010.

- 
- Samuel S Shapiro and RS Francia. An approximate analysis of variance test for normality. *Journal of the American Statistical Association*, 67(337):215–216, 1972.
- Samuel Sanford Shapiro and Martin B Wilk. An analysis of variance test for normality (complete samples). *Biometrika*, 52(3/4):591–611, 1965.
- Joseph P Simmons, Leif D Nelson, and Uri Simonsohn. False-positive psychology: Undisclosed flexibility in data collection and analysis allows presenting anything as significant. *Psychological science*, 22(11):1359–1366, 2011.
- Casper Kaae Sønderby, Tapani Raiko, Lars Maaløe, Søren Kaae Sønderby, and Ole Winther. Ladder variational autoencoders. In *Proceedings of the 30th International Conference on Neural Information Processing Systems*, pp. 3745–3753, 2016.
- Michael A Stephens. *Goodness-of-fit techniques*. Routledge, 2017.
- David L Streiner. Best (but oft-forgotten) practices: the multiple problems of multiplicity—whether and how to correct for many statistical tests. *The American journal of clinical nutrition*, 102(4): 721–728, 2015.
- Ilya Tolstikhin, Olivier Bousquet, Sylvain Gelly, and Bernhard Schoelkopf. Wasserstein auto-encoders. *arXiv preprint arXiv:1711.01558*, 2017.
- Michael Tschannen, Olivier Bachem, and Mario Lucic. Recent advances in autoencoder-based representation learning. *arXiv preprint arXiv:1812.05069*, 2018.
- Arash Vahdat and Jan Kautz. Nvae: A deep hierarchical variational autoencoder. *arXiv preprint arXiv:2007.03898*, 2020.
- Cédric Villani. *Optimal transport: old and new*, volume 338. Springer Science & Business Media, 2008.
- Tianlin Xu, Li Kevin Wenliang, Michael Munn, and Beatrice Acciaio. Cot-gan: Generating sequential data via causal optimal transport. *Advances in Neural Information Processing Systems*, 33:8798–8809, 2020.